

UC Davis

UC Davis Previously Published Works

Title

ECM-dependent HIF induction directs trophoblast stem cell fate via LIMK1-mediated cytoskeletal rearrangement.

Permalink

<https://escholarship.org/uc/item/5vk5p0nt>

Journal

PLoS ONE, 8(2)

Authors

Choi, Hwa

Sanders, Timothy

Tormos, Kathryn

et al.

Publication Date

2013

DOI

10.1371/journal.pone.0056949

Peer reviewed

ECM-Dependent HIF Induction Directs Trophoblast Stem Cell Fate via LIMK1-Mediated Cytoskeletal Rearrangement

Hwa J. Choi¹, Timothy A. Sanders¹, Kathryn V. Tormos^{1,4}, Kurosh Ameri¹, Justin D. Tsai¹, Angela M. Park¹, Julissa Gonzalez², Anthony M. Rajah¹, Xiaowei Liu^{3,4}, Diana M. Quinonez², Paolo F. Rinaudo^{3,4}, Emin Maltepe^{1,4,5,6*}

1 Department of Pediatrics, University of California San Francisco, San Francisco, California, United States of America, **2** Department of Biology, San Francisco State University, San Francisco, California, United States of America, **3** Department of Obstetrics, Gynecology and Reproductive Sciences, University of California San Francisco, San Francisco, California, United States of America, **4** Center for Reproductive Sciences, University of California San Francisco, San Francisco, California, United States of America, **5** Eli and Edythe Broad Center of Regeneration Medicine and Stem Cell Research, University of California San Francisco, San Francisco, California, United States of America, **6** Developmental and Stem Cell Biology Program, University of California San Francisco, San Francisco, California, United States of America

Abstract

The Hypoxia-inducible Factor (HIF) family of transcriptional regulators coordinates the expression of dozens of genes in response to oxygen deprivation. Mammalian development occurs in a hypoxic environment and HIF-null mice therefore die in utero due to multiple embryonic and placental defects. Mouse embryonic stem cells do not differentiate into placental cells; therefore, trophoblast stem cells (TSCs) are used to study mouse placental development. Consistent with a requirement for HIF activity during placental development in utero, TSCs derived from HIF-null mice exhibit severe differentiation defects and fail to form trophoblast giant cells (TGCs) *in vitro*. Interestingly, differentiating TSCs induce HIF activity independent of oxygen tension via unclear mechanisms. Here, we show that altering the extracellular matrix (ECM) composition upon which TSCs are cultured changes their differentiation potential from TGCs to multinucleated syncytiotrophoblasts (SynTs) and blocks oxygen-independent HIF induction. We further find that modulation of Mitogen Activated Protein Kinase Kinase-1/2 (MAP2K1/2, MEK-1/2) signaling by ECM composition is responsible for this effect. In the absence of ECM-dependent cues, hypoxia-signaling pathways activate this MAPK cascade to drive HIF induction and redirect TSC fate along the TGC lineage. In addition, we show that integrity of the microtubule and actin cytoskeleton is critical for TGC fate determination. HIF-2 α ensures TSC cytoskeletal integrity and promotes invasive TGC formation by interacting with c-MYC to induce non-canonical expression of *Lim domain kinase 1*—an enzyme that regulates microtubule and actin stability, as well as cell invasion. Thus, we find that HIF can integrate positional and metabolic cues from within the TSC niche to regulate placental development by modulating the cellular cytoskeleton via non-canonical gene expression.

Citation: Choi HJ, Sanders TA, Tormos KV, Ameri K, Tsai JD, et al. (2013) ECM-Dependent HIF Induction Directs Trophoblast Stem Cell Fate via LIMK1-Mediated Cytoskeletal Rearrangement. PLoS ONE 8(2): e56949. doi:10.1371/journal.pone.0056949

Editor: Adam J. Engler, University of California, San Diego, United States of America

Received: October 9, 2012; **Accepted:** January 16, 2013; **Published:** February 21, 2013

Copyright: © 2013 Choi et al. This is an open-access article distributed under the terms of the Creative Commons Attribution License, which permits unrestricted use, distribution, and reproduction in any medium, provided the original author and source are credited.

Funding: The research was made possible by a grant from the California Institute for Regenerative Medicine (Grant Number TB1-01194) and the National Institutes of Health (HL087754, HD072455). The funders had no role in study design, data collection and analysis, decision to publish, or preparation of the manuscript.

Competing Interests: The authors have declared that no competing interests exist.

* E-mail: emin.maltepe@ucsf.edu

Introduction

Mammalian development occurs in a physiologically hypoxic environment that drives the expression of dozens of genes via the Hypoxia-inducible Factor (HIF) family of transcriptional regulators [1]. A heterodimeric transcription factor composed of alpha and beta subunits, HIF can activate canonical target genes in response to oxygen deprivation by directly binding to hypoxia response elements (HRE) located within their regulatory regions [2,3]. Due to the short half-life of alpha subunits, HIF activity can be tightly regulated [4]. Mitochondrial oxygen sensing mechanisms produce highly labile reactive oxygen species to ensure that HIF- α subunit stabilization occurs only under hypoxic conditions [5]. Oxygen gradients that are generated as a function of tissue growth can thus activate HIF in a dynamic fashion to pattern the

developing embryo [6]. Consistent with this, HIF activity is required for embryonic development [7,8,9].

During mammalian gestation, the placenta forms a vital transport interface between the maternal and fetal circulations and its development is also dependent on HIF activity [10,11,12,13]. In mice, two terminally differentiated cell types are primarily responsible for placental function: 1. trophoblast giant cells (TGC) and, 2. multinucleated syncytiotrophoblasts (SynT) [14]. TGCs anchor the placenta to the uterus and direct maternal blood flow to the conceptus while SynTs perform the transport functions of the placenta [15]. The derivation of trophoblast stem cells (TSCs) that differentiate into these placental cells *in vitro* has enhanced our understanding of placental development *in vivo* [16]. Interestingly, however, TSC differentiation using conventional techniques results primarily in the

production of TGCs that is associated with the stabilization of HIF- α subunits independent of oxygen tension [10,17]. We previously demonstrated that HIF induction is critical for TGC differentiation as *Hif-1/2 α* ^{-/-} (compound null) or *Hif-1 β* (*Arnt*)^{-/-} TSCs (collectively referred to as HIF-null) fail to produce TGCs *in vitro*, differentiating primarily into multinucleated SynTs, indicating that HIF activity can suppress cell fusion and SynT fate determination [10,17]. The mechanisms responsible for differentiation-dependent HIF induction and how HIF ultimately regulates cell fate in the placenta remain unknown, however.

Here, we show that TSC-extracellular matrix (ECM) interactions provide positional cues during normoxia that trigger differentiation-dependent HIF induction via signaling pathways that intersect with metabolic responses to oxygen deprivation. We find that altering the ECM substrate upon which TSCs are cultured impacts differentiation-dependent HIF stabilization and TSC fate. SynT formation is dependent on cell fusion – a process that is associated with significant cytoskeletal reorganization [18,19] [20,21]. Consistent with this, HIF-null TSCs exhibit dramatic morphological changes upon syncytialization [17]. We now show that non-canonical HIF-2 activity, induced in response to hypoxia or ECM composition, can prevent this process by promoting *Limk1* expression and subsequent cytoskeletal stabilization.

Results

ECM Composition Regulates TSC Fate and HIF Stability Independent of O₂ Tension

TSC proliferation depends on Fibroblast Growth Factor 4 (FGF4) as well as the presence of fibroblast “feeder” cells or fibroblast conditioned medium (Fib-CM) [16]. In the absence of either, TSCs default to a TGC differentiation program. While screening for culture conditions that could maintain FGF4-dependent TSC growth independent of fibroblasts or Fib-CM, we identified the xeno-free defined ECM substrate, CELLstartTM (Invitrogen) [22,23]. This ECM substrate is composed primarily of Fibronectin, along with other ECM components [24], and thus represents a physiologically relevant substrate for TSC culture [25,26]. TSCs maintained on CELLstartTM in the presence of FGF4, but without fibroblasts or Fib-CM, proliferated indefinitely and expressed TSC-specific transcription factors such as CDX2 and EOMES [16](Fig. 1A–D), the levels of which dramatically decreased following FGF4 withdrawal (not shown). Interestingly, however, differentiation in 21% O₂ (room air) following FGF4 withdrawal of TSCs maintained on CELLstartTM promoted cell fusion and resulted primarily in the formation of multinucleated SynTs (Fig. 1E, 1F), as opposed to the TGCs commonly observed with TSCs maintained on fibroblasts or on TC plastic in Fib-CM [16,17]. Importantly, differentiation under hypoxic (2% O₂) conditions could reverse this cell fate choice (Fig. 1G, 1H), blocking SynT formation and generating TGCs expressing the lineage specific transcription factor HOPX1 [27]. Lineage-specific gene expression analyses further confirmed that wild-type TSCs differentiated following culture on CELLstartTM expressed dramatically reduced levels of the TGC-specific markers *Placental lactogens I* and *-2*, *Proliferin* and *Cathepsin Q*, and exhibited increased levels of the SynT markers *Tfeb* and *SynA*, when compared with genetically identical TSCs differentiated following culture on TC plastic in Fib-CM (Fig. 1I). Importantly, this pattern of gene expression was similar to, though more pronounced than, that observed following differentiation of *Arnt*^{-/-} or *Hif-1/2 α* ^{-/-} TSCs that form SynTs following culture on TC plastic in Fib-CM (Fig. 1I) [10] [17]. We therefore asked whether the alteration of

TSC fate following culture on CELLstartTM might be due to impaired HIF- α subunit stabilization that normally occurs during differentiation using standard techniques [17]. Indeed, TSCs differentiated following culture on CELLstartTM in 21% O₂ failed to stabilize HIF-2 α and only slightly accumulated HIF-1 α protein levels, whereas differentiation in 2% O₂ induced both proteins (Fig. 1J). Furthermore, TSCs derived from *Vhlh*^{-/-} embryos, which exhibit constitutively elevated HIF-1 α and -2 α due to lack of VHL-dependent ubiquitination and proteasomal degradation [2,3], still formed TGCs in 21% O₂ following differentiation despite maintenance on CELLstartTM (Fig. 1K). These results suggest that TSC derivation on fibroblasts and maintenance on TC plastic in Fib-CM provides a set of extracellular cues that promote O₂-independent HIF stabilization and subsequent TGC formation during differentiation that are lost when TSCs are maintained on the defined ECM substrate, CELLstartTM. To understand the mechanisms responsible, we concentrated on cell surface integrin expression, as these molecules play a central role in cell-ECM interactions [28]. TSCs maintained on CELLstartTM were compared with TSCs maintained on TC plastic in Fib-CM. Interestingly, culture on CELLstartTM completely blocked β 3-integrin expression in both undifferentiated and differentiated TSCs (Fig. 2A–D), suggesting that ECM composition determines cell surface integrin expression and thereby modulates downstream signaling and TSC fate. Importantly, while undifferentiated TSCs maintained on TC plastic in Fib-CM expressed this β 3-integrin, its cell surface expression was largely restricted to differentiated TGCs, consistent with HIF induction being associated with TGC differentiation.

ECM- and Oxygen-dependent HIF Stabilization and TGC Formation Occur via MAP2K1/2-dependent Signaling

We suspected that candidate pathways capable of integrating ECM-dependent signals with oxygen-dependent inputs might include members of the mitogen activated protein kinase (MAPK) cascade. This is due to the fact each set of stimuli can independently activate this signaling cascade [29] [30,31,32,33]. Consistent with this, pharmacological inhibition of MAP2K1/2 (MEK-1/2) activity prevented HIF- α subunit stabilization during hypoxic (2% O₂) differentiation of TSCs cultured on CELLstartTM (Fig. 3A) and during normoxic (21% O₂) differentiation following culture on TC plastic in Fib-CM (Fig. 3B). Furthermore, hypoxic TGC formation of TSCs following culture on CELLstartTM could be suppressed with the same MAP2K1/2 inhibitor (Fig. 3C–E), while transient expression of constitutively active MAP2K1 (Fig. 3F) promoted TGC formation under normoxic conditions and dominant negative MAP2K1 allowed cell fusion under hypoxic conditions (Fig. 3G). And finally, pharmacological MAP2K1/2-inhibition could prevent TGC formation and promoted SynT differentiation in TSCs that had been cultured on TC plastic in Fib-CM (Fig. 3H, 3I). Northern blot analysis confirmed that MAP2K1/2 inhibition in wild-type TSCs suppressed expression of the TGC as well as spongiotrophoblast (SpT) marker genes, *Placental lactogen I* and *4311*, respectively, nearly to levels observed in differentiated *Arnt*^{-/-} TSCs (Fig. 3J). Collectively, these results confirm that ECM- and oxygen-dependent HIF- α subunit stabilization and subsequent TGC formation occurs through a MAP2K1/2-dependent pathway.

Cytoskeletal Rearrangement is Central to MAP2K1/2-mediated TGC Formation

Similar to mitochondrial responses to changing O₂ levels, dynamic integrin ligation in response to changes in ECM

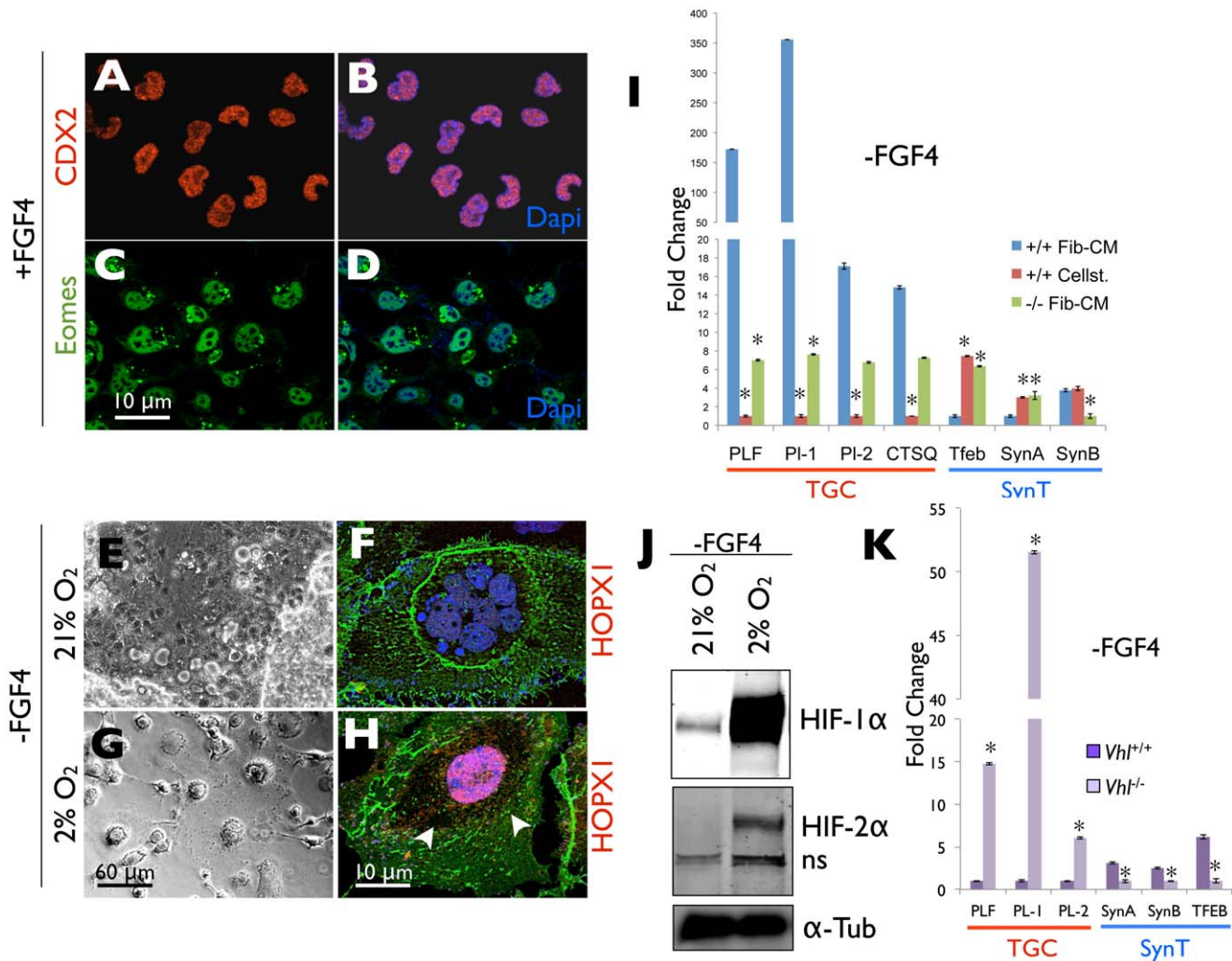


Figure 1. HIF integrates ECM cues and Oxygen Levels to Direct TSC Fate. (A–D) Immunofluorescence microscopy of undifferentiated control TSCs cultured on CELLstart™ with anti-CDX2 and EOMES antibodies (blue = DAPI, red = CDX2, green = Eomes). (E, G) Phase contrast microscopy of control TSCs maintained on CELLstart™ following differentiation for 7 days under normoxic (21% O₂) or hypoxic (2% O₂) conditions. (F, H) Immunofluorescence microscopy of control TSCs maintained on CELLstart™ following differentiation for 7 days under normoxic (21% O₂) or hypoxic (2% O₂) conditions with an anti-HOPX1 (red) antibody (blue = DAPI). (I) Quantitative RT-PCR analysis of *Pl. I*, *Pl.II*, *Ctsq*, *Plf*, *Tfeb*, *SynA* and *SynB* gene expression in wild-type (+/+) TSCs differentiated for 7 days following culture on CELLstart™ or on TC plastic in Fib-CM, compared with *Arnt*^{-/-} (-/-) TSCs differentiated following culture on TC plastic in Fib-CM. p values <0.05 versus wild-type Fib-CM indicated by an asterisk. (J) Immunoblot of HIF-1α and -2α protein levels in whole cell lysates of wild-type TSCs differentiated for 7 days following culture on CELLstart™ at 21% O₂ or 2% O₂. (K) Quantitative RT-PCR analysis of *Pl-1*, *Pl-2*, *Plf*, *Tfeb*, *SynA* and *SynB* expression in *Vhlh*^{+/+} and *Vhlh*^{-/-} TSCs differentiated following culture on CELLstart™. p values <0.05 versus wild-type indicated by an asterisk. doi:10.1371/journal.pone.0056949.g001

composition allow a cell to sense its environment by converting positional information into downstream signals [34]. These frequently result in cytoskeletal reorganization [35] that can promote cell migration or other alterations in cell behavior [36]. Additionally, trophoblast differentiation has been associated with significant cytoskeletal changes [19,20,37]. We therefore examined the cytoskeletal organization of differentiated control and *Hif-1/2α*^{-/-} TSCs that had been maintained on TC plastic in Fib-CM and analyzed its association with MAP2K1/2 activation. TGCs derived from control TSCs contained robust MTs extending the length of the cell (Fig. 4A, 4D), while multinucleated SynTs derived from *Hif-1/2α*^{-/-} TSCs exhibited a disrupted microtubule (MT) network consisting of “broken” appearing MT fragments (Fig. 4B arrows, 4F). MT integrity associated strongly with MAP2K1/2 activity, as control TGCs with robust MTs

stained strongly for the phosphorylated versions of the MAP2K1/2 target MAPK3/1 (ERK-1/2) (Fig. 4A), while multinucleated SynTs derived from *Hif-1/2α*^{-/-} TSCs did not (Fig. 4B). Only unfused SynT progenitors that did not contain “broken” MTs continued to exhibit the active form of this kinase in *Hif-1/2α*^{-/-} TSCs (Fig. 4B, arrowheads). Additionally, we observed dramatic differences in the actin cytoskeleton, with robust stress fibers noted in TGCs (Fig. 4C) while SynTs exhibited a disorganized actin cytoskeleton containing high amounts of diffusely distributed F-actin (Fig. 4E). To formally test whether cytoskeletal integrity could regulate TSC fate, we investigated whether pharmacological MT or actin disrupting agents could promote SynT formation of TSCs cultured using conventional techniques. Indeed, the MT disrupting agent Taxol (Paclitaxel) (Fig. 4G) and the actin disrupting agent cytochalasin B (Fig. 4H) inhibited TGC

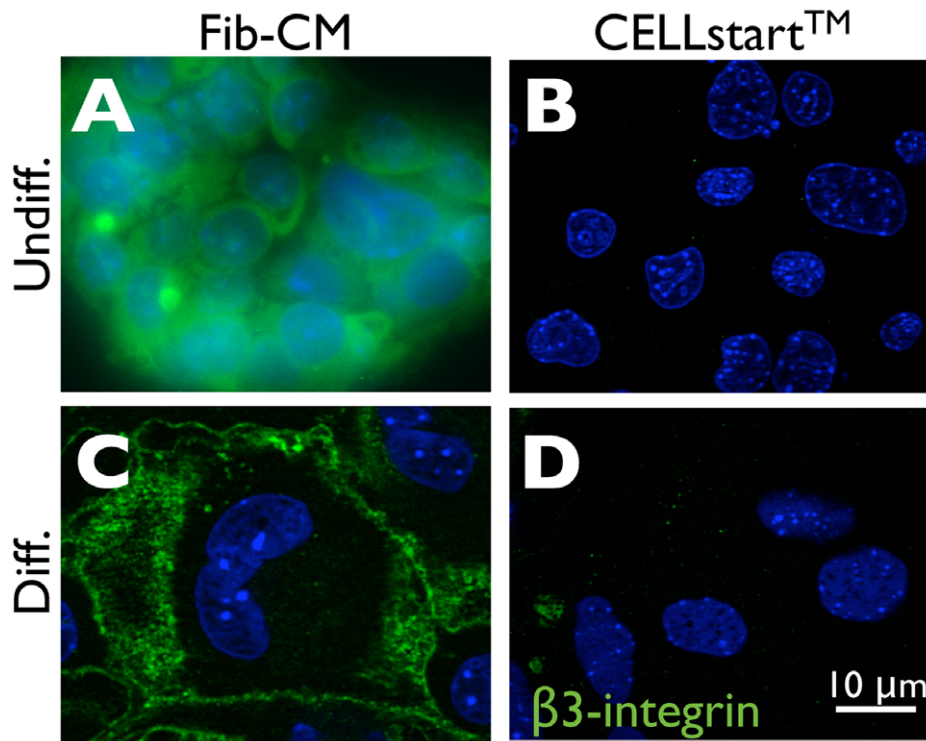


Figure 2. β -Integrin (CD61) is downregulated in TSCs following culture on CELLstart™. Immunofluorescence microscopy of wild-type TSCs maintained on TC plastic in Fib-CM (A) or on CELLstart™ (B) in the presence of FGF4 and heparin (Undiff.) or following differentiation (Diff., C and D) using an anti-CD61 antibody (green) (magnification 630X). doi:10.1371/journal.pone.0056949.g002

formation and promoted the formation of multinucleated SynTs in control TSCs that had been maintained on TC plastic in Fib-CM.

HIF-dependent *Limk1* Expression Promotes TGC Differentiation

We next focused our efforts on identifying cytoskeleton regulatory molecules that may be misregulated in the absence of HIF activity. Gene array studies indicated that expression of the gene encoding Lim domain kinase 1 (LIMK1), an enzyme responsible for regulating MT and Actin integrity [38], was significantly downregulated in the absence of HIF activity (not shown). Immunofluorescence microscopy confirmed that HIF-null TS cells differentiated into SynTs expressed no detectable LIMK1 expression, while control TGCs expressed robust LIMK1 protein levels in a perinuclear distribution (compare Fig. 5A and 5B). Immunoblot analyses confirmed this (see below) and indicated that the MAP2K1/2 inhibitor U0126 significantly decreased LIMK1 levels in wild-type TSCs differentiated following maintenance on TC plastic in Fib-CM (Fig. 5H), consistent with its ability to block HIF stabilization during differentiation. Furthermore, we found that the LIMK1 target Cofilin was highly phosphorylated, also in a perinuclear distribution, and therefore inactive in TGCs (Fig. 5D), but not in SynTs (Fig. 5E), which frequently contained prominent Cofilin rods that form when Cofilin is hyperactive [39] (Fig. 5E, arrowheads). The residual phosphorylation of Cofilin rods in SynTs may be due to their residual low-level LIMK2 levels (see below) [38]. Furthermore, transient LIMK1 expression in differentiating *Hif-1/2 α ^{-/-}* TSCs promoted the appearance of large TGCs in the majority of transfected cells, as opposed to the SynTs commonly observed following their differentiation (Fig. 5F, 5G). These results suggest that HIF-dependent LIMK1 expression

can regulate TSC fate downstream of ECM- or oxygen-dependent MAP2K1/2 activation by modulating the cytoskeleton.

Non-Canonical HIF-2 α Activity Drives TSC Fate via LIMK1-mediated Cytoskeletal Stabilization

We next investigated how HIF regulates *Limk1* gene expression during TSC differentiation. We first determined whether we could detect canonical HIF-DNA interactions in differentiated TSCs via electrophoretic mobility shift assays (EMSA). As seen, control TSCs maintained on TC plastic in Fib-CM and differentiated in room air (21% O₂) contained abundant HRE-bound HIF complexes (Fig. 6A), consistent with our prior observations of HIF activation during normoxic differentiation of TSCs maintained using conventional methods [13]. Interestingly, however, while two different HIF-1 α -specific antibodies produced a “super-shift, SS” in differentiated TSC nuclear extracts, a HIF-2 α -specific antibody did not (Fig. 6A), suggesting that HIF-1 α was predominantly responsible for canonical HRE-mediated gene expression in differentiating TSCs. To interrogate the requirement for direct HIF-DNA binding during TSC fate determination, we stably reconstituted *Hif-1/2 α ^{-/-}* TSCs [10] utilizing a PiggyBac transposon system [40] either with HA-tagged wild-type HIF-1 α or HIF-2 α individually, or with mutant forms of each lacking their DNA binding basic domains (HIF-1 α Δ b, HIF-2 α Δ b) (Fig. 6B). Deletion of the basic domain prevents HRE binding and canonical target gene expression by HIF complexes without affecting their stability [41]. As expected, full-length versions of each were capable of activating their respective canonical downstream target genes in HIF-null TSCs, while versions lacking their basic domains could not (Fig. 6C, 6D).

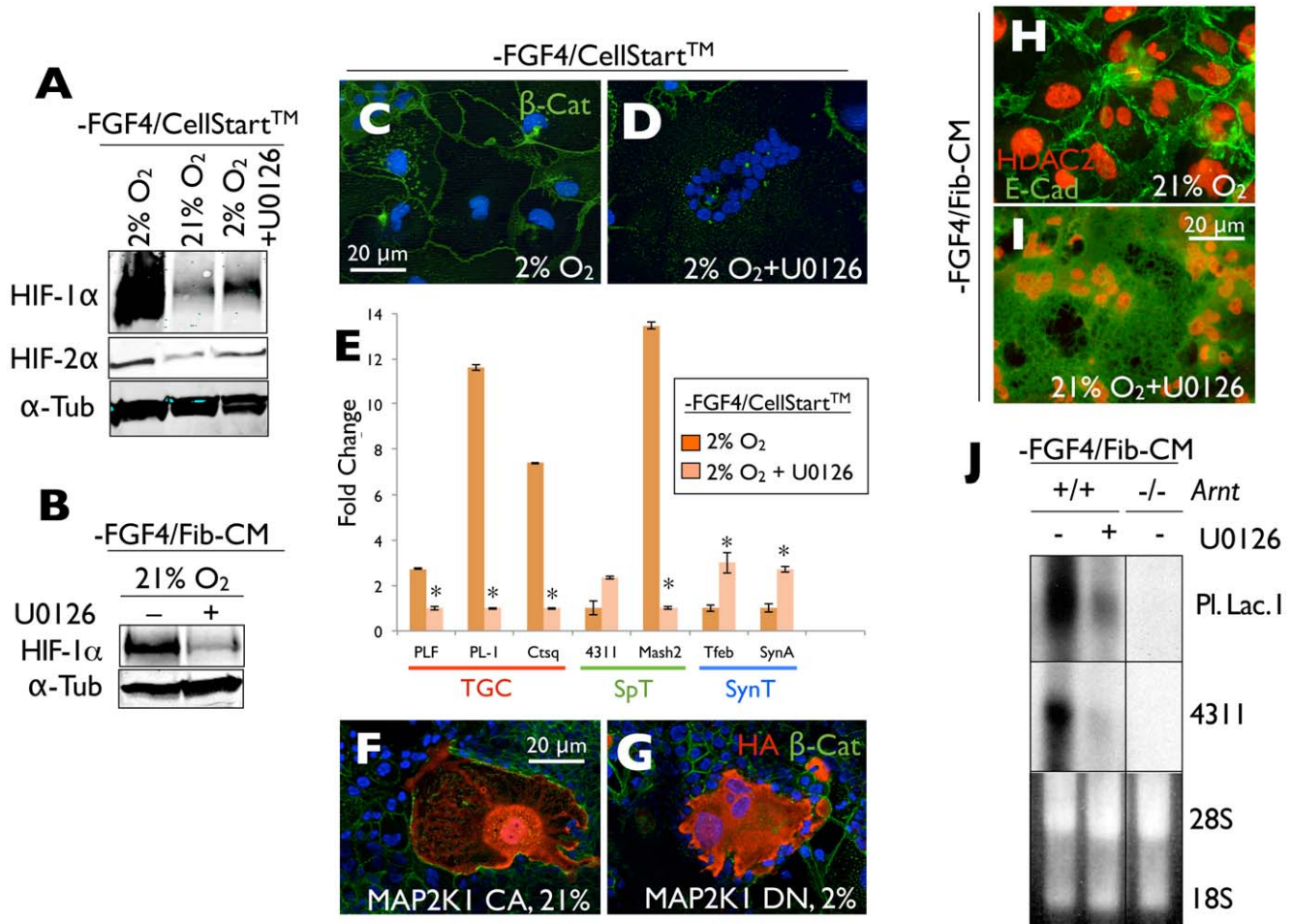


Figure 3. ECM- or oxygen-dependent HIF- α subunit stabilization and TGC formation are dependent on MAP2K1/2 activity. (A) Immunoblot of whole cell lysates obtained from TSCs differentiated in 2% or 21% O₂, with and without U0126, following culture on CELLstart™, for HIF-1 α , -2 α or α -Tubulin. (B) Immunoblot of whole cell lysates obtained from differentiated wild-type TSCs following culture on TC plastic in Fib-CM with and without U0126 with a HIF-1 α antibody. (C) (D) Immunofluorescence microscopy of TSCs maintained on CELLstart™ following differentiation for 7 days under hypoxic conditions without and with U0126 (10 μ M) using anti β -Catenin antibodies (green) (blue = Dapi). (E) Quantitative RT-PCR analysis of *Plf*, *Pl-I*, *Ctsq*, *4311*, *Mash2*, *Tfeb* and *SynA* expression following differentiation of wild-type TSCs cultured on CELLstart™ under hypoxic conditions without and with U0126. p values <0.05 versus drug free control indicated by an asterisk. (F) Immunofluorescence microscopy using anti HA (red) and β -Catenin (green) antibodies of control TSCs differentiated following culture on CELLstart™ under 21% O₂ following transient transfection with constitutively active HA:MAP2K1 or under (G) 2% O₂ following transient transfection with dominant negative HA:MAP2K1. (H, I) Immunofluorescence microscopy of wild-type TSCs differentiated following culture on TC plastic in Fib-CM in 21% O₂ with and without U0126 with antibodies for HDAC2 (red) and E-Cadherin (green). (J) Northern blot analysis of lineage specific marker gene expression in wild-type TSCs maintained on TC plastic in Fib-CM and differentiated with and without U0126, compared with differentiated *Arnt*^{-/-} TSCs.
doi:10.1371/journal.pone.0056949.g003

Using this system, we investigated the HIF- α subunit dependence of LIMK1 expression. Interestingly, while neither HIF-1 α nor HIF-1 $\alpha\Delta b$ restored LIMK1 protein levels in *Hif-1/2 α* ^{-/-} TSCs to that observed in wild-type TSCs, both HIF-2 α and HIF-2 $\alpha\Delta b$ did (Fig. 7A, 7B), suggesting it to be a non-canonical HIF-2-specific target gene. We suspected that the HIF-2-specificity may be due to its known interaction with and activation of c-MYC-dependent transcription [42,43]. To test this, we immunoprecipitated HA-tagged HIF-2 $\alpha\Delta b$ in reconstituted *Hif-1/2 α* ^{-/-} TSCs and detected strong c-MYC interaction (Fig. 7C). We next identified a 100% conserved c-MYC binding E box (CACGTG) in the *Limk1* promoter, but no canonical HIF binding sites, and detected both c-MYC as well as HIF-2 α binding to this site *in situ* in differentiated TGCs by chromatin immunoprecipitation (Fig. 7D). We then tested whether pharmacological c-MYC inhibition could block non-

canonical HIF-2 α -dependent *Limk1* gene expression, and found that it could decrease LIMK1 protein levels in HIF-2 $\alpha\Delta b$ expressing cells (Fig. 7E). This indicates that HIF-2 α interacts with c-MYC containing transcriptional complexes during TSC differentiation and that this interaction contributes to *Limk1* expression during TGC differentiation (Fig. 7F). Stable HIF-2 $\alpha\Delta b$ expressing HIF-null TSCs, whether cultured on CELLstart or on TC plastic in Fib-CM, failed to fuse into multinucleated SynTs and differentiated along the TGC lineage (Fig. 8A, 8B, 8C). Importantly, pharmacological cytoskeleton disruption (Fig. 8D, 8F, 8G) could reverse this effect, promoting SynT formation in these cells. Additionally, pharmacological LIMK1 inhibition [44,45] promoted the formation of multinucleated cells (Fig. 8E, 8H) in HIF-null TSCs reconstituted with HIF-2 $\alpha\Delta b$.

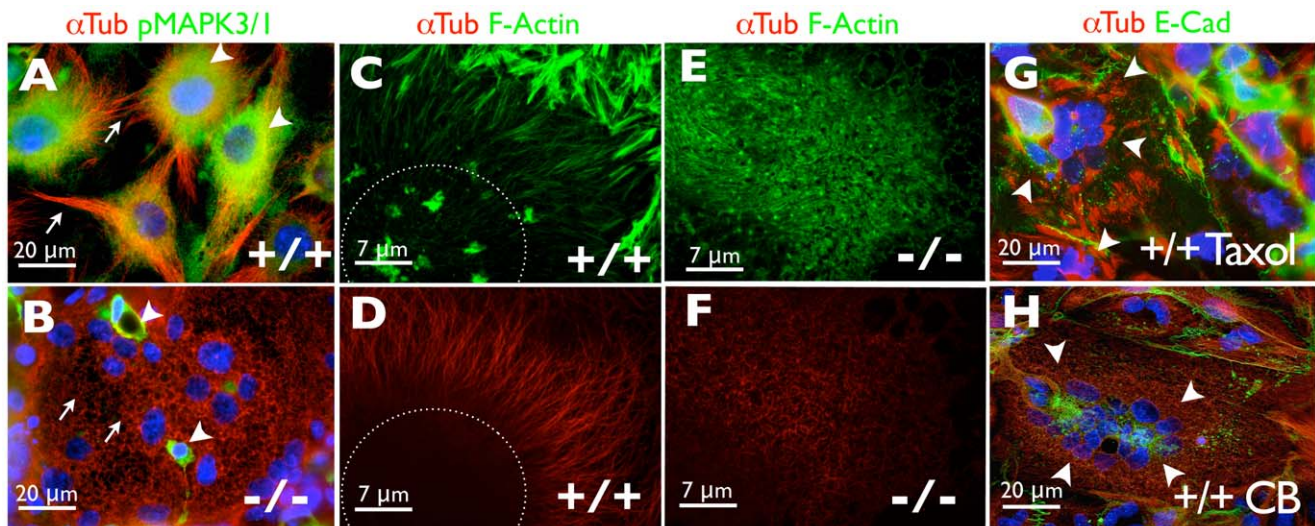


Figure 4. MAP2K1/2 inhibition and cytoskeletal rearrangement in differentiating HIF-null TSCs. Immunofluorescence microscopy of terminally differentiated wild-type (+/+) TGCs (A) and *Hif-1/2 α ^{-/-}* (-/-) SynTs (B) with an anti α -Tubulin (red), or p-MAPK3/1 (green) antibody (arrows = microtubules, arrowheads = pMAPK3/1). (C) Confocal microscopy imaging of polymerized actin via FITC-phalloidin staining (green) or (D) α -Tubulin (red) in terminally differentiated control TGCs (dashed line indicates approximate location of nucleus). (E) Confocal microscopy imaging of polymerized actin via FITC-phalloidin staining (green) or (F) α -Tubulin (red) in terminally differentiated HIF-null SynTs. (G) Differentiation of control TGCs in the presence of Taxol (G) or (H) Cytochalasin B (CB) promoted the formation of multinucleated cells (arrowheads) following culture on TC plastic in Fib-CM. α -Tubulin (red) and E-Cadherin (green). doi:10.1371/journal.pone.0056949.g004

Discussion

Collectively, our results indicate that oxygen- and canonical target gene-independent HIF activity can drive TSC fate in response to positional cues encoded by ECM components within the TSC microenvironment (Fig. 9). Initially thought to function as a mere scaffold, the ECM is now known to regulate many aspects of cell behavior, including proliferation and growth, survival, migration, and differentiation [28,46]. Primary components of the ECM are structural proteins (e.g., collagens, laminins, fibronectin, vitronectin and elastin) and specialized glycoproteins that can interact with molecules having important biological functions such as growth factors. The precise composition varies by location. In the stem cell niche, the ECM can provide instructive cues for cell fate decisions via the integrin family of heterodimeric cell surface receptors [26,47,48]. In erythropoiesis, for example, adhesion of primary erythroid progenitors to fibronectin mediated by $\alpha_4\beta_1$ integrin is necessary for proper proliferation *in vitro* [49]. In this system, signals from the ECM cooperate with signals from the soluble factor erythropoietin to activate pathways necessary for terminal differentiation and proliferation. In TSCs, altering their ECM in this way alters their cell surface β_3 -integrin expression, and subsequent HIF induction during differentiation. We have shown here that in TSCs, altering their ECM in this way alters their cell surface β_3 -integrin expression, and subsequent HIF induction during differentiation. Supporting a link between HIF activity and ECM-dependent integrin ligation, $\alpha\beta_3$ activation can trigger HIF accumulation in some cancer cells [50] and HIF-deficiency negatively affects TSC surface β_3 -integrin localization [51], suggesting that HIF- α subunit stability can both be activated by, as well as further promote, cell surface integrin activity. Importantly, trophoblast adhesion to ECM is governed by integrins [52–53] and hypoxic conditions promote trophoblast invasion in utero [54].

The mitogen activated protein kinase (MAPK) cascade is a frequent point of convergence from multiple environmental inputs

[35,55]. We therefore reasoned that candidate signaling pathways responsible for oxygen-dependent HIF induction that could interface with ECM-dependent signaling would include members of this family. The classical extracellular regulated kinase (ERK)/MAPK signaling pathway is an obvious candidate because it: 1. Regulates cell fate in a broad range of organisms [56,57,58,59]; 2. Responds to hypoxia downstream of mitochondrial ROS [60] and, 3. Is activated by integrin ligation [61]. Importantly, in mice, MEK1 (renamed MAP2K1), as well as its downstream target ERK2 (renamed MAPK1), are critical regulators of placentation [62,63,64,65]. Interestingly, MAP2K1 deficiency results in placental malformation characterized by an excess of multinucleated cells within affected placentas *in vivo* [66], similar to the formation of multinucleated SynTs with HIF-deficient TSCs *in vitro*, while genetic disruption of the MAP3K B-Raf results in placental malformation associated with diminished HIF-1 α protein levels [67], consistent with our results.

Our results also shed novel insights into HIF-dependent cell fate determination. We found that HIF-2 α can interact with c-MYC to enhance *Limk1* gene expression and promote cytoskeletal integrity, thereby enhancing TGC differentiation, via non-canonical means. While HIF-2 α has previously been shown to activate c-MYC-dependent target genes [42,43], to our knowledge this is the first demonstration of a role for this mechanism during normal placentation in mice [68]. Also, while HIF activity is generally assumed to result from the reduced oxygen tension frequently encountered during development, our results provide evidence that ECM composition can be added to a growing list of O₂-independent factors that can also drive HIF-dependent developmental programs such as Insulin-like Growth Factor 1 [69], or Runx2-mediated HIF stabilization [70]. Additionally, we show that the dramatic cytoskeletal changes observed in SynTs are not a simple by-product of cell fusion, but help regulate cell fate decisions in the placenta. LIMK1 is likely activated downstream of Rho kinase which is known to be induced during TGC formation

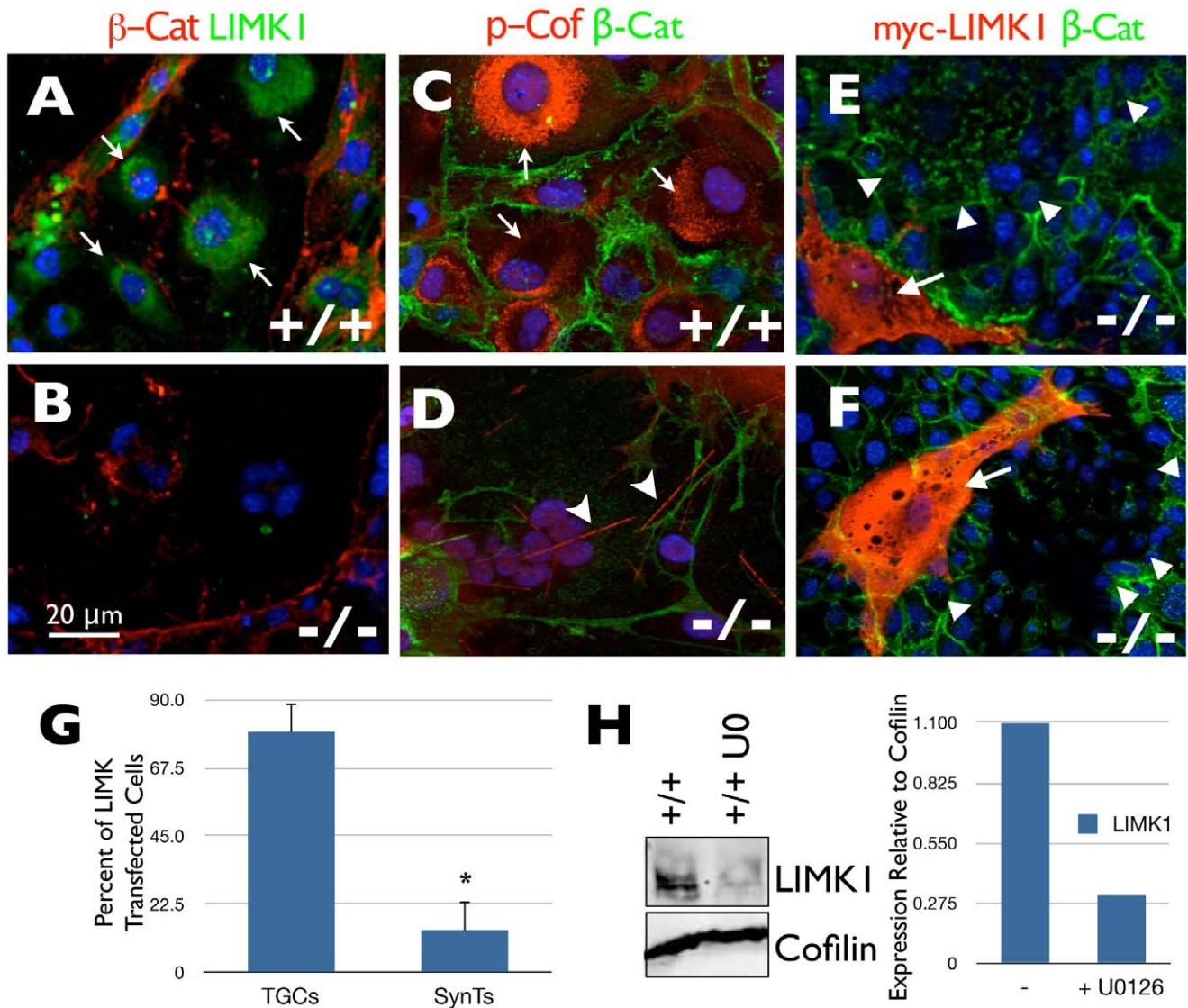


Figure 5. HIF-dependent LIMK1 expression promotes TGC formation in TSCs. Immunofluorescence microscopy of terminally differentiated control TGCs (A) and *Hif-1/2 α ^{-/-}* SynTs (B) with a β -Catenin (red) and LIMK1 (green) antibody (arrows=perinuclear LIMK1 staining). Immunofluorescence microscopy of terminally differentiated control TGCs (C) and *Hif-1/2 α ^{-/-}* SynTs (D) with a β -Catenin (green) and p-Cofilin (red) antibody (arrows=perinuclear p-Cof staining, arrowheads=cofilin rods). (E, F) Two representative images of TGC formation (arrows) following transient myc-LIMK1 expression in *Hif-1/2^{-/-}* TSCs while untransfected cells primarily form SynTs (arrowheads) (red = myc-LIMK1, green = β -catenin). (G) Quantification of the percentage of LIMK1 transfected HIF-null TSCs differentiated into TGCs vs. SynTs. (H) Immunoblot analysis of LIMK1 levels in differentiated wild-type (+/+) TSCs without and with U0126 (U0). Integrated densitometry confirmed the decreased expression of LIMK1, relative to total Cofilin, in control TSCs differentiated in the presence of U0126. doi:10.1371/journal.pone.0056949.g005

[37]. Interestingly, HIF stability can be influenced by MT integrity [71,72], suggesting the possibility of a feed-forward mechanism whereby MAPK-dependent HIF activity promotes MT integrity, which further enhances HIF stability during TGC differentiation.

In addition to playing important roles during normal placental development, the pathway outlined here is likely to be involved in pregnancy complications such as preeclampsia wherein fetal trophoblasts fail to properly invade maternal tissues. While aberrant oxygenation and HIF activity have previously been associated with preeclampsia [73,74], its ability to regulate LIMK1 has particular relevance, given that LIMK1 has recently been shown to be important for tumor cell invasion in humans [44] as well as collective cell migration in *D. melanogaster* [75]. Furthermore, in addition to altered hypoxia signaling, ECM remodeling is

also frequently disrupted in PE [76], suggesting novel roles for HIF in linking these disparate processes. Further investigation of the intersection of these pathways by HIF activation should therefore yield novel insights into the etiology of this intractable syndrome.

Methods

TSC Culture

Mouse TSCs were derived on human placental fibroblasts as previously described [17]. Prior to differentiation experiments, TSCs were subjected to a differential plating to remove fibroblasts and subsequently cultured for two passages in 70% Fib-CM with FGF4 and heparin [16]. Differentiations were performed in standard TSC medium without FGF4 or heparin, on tissue culture

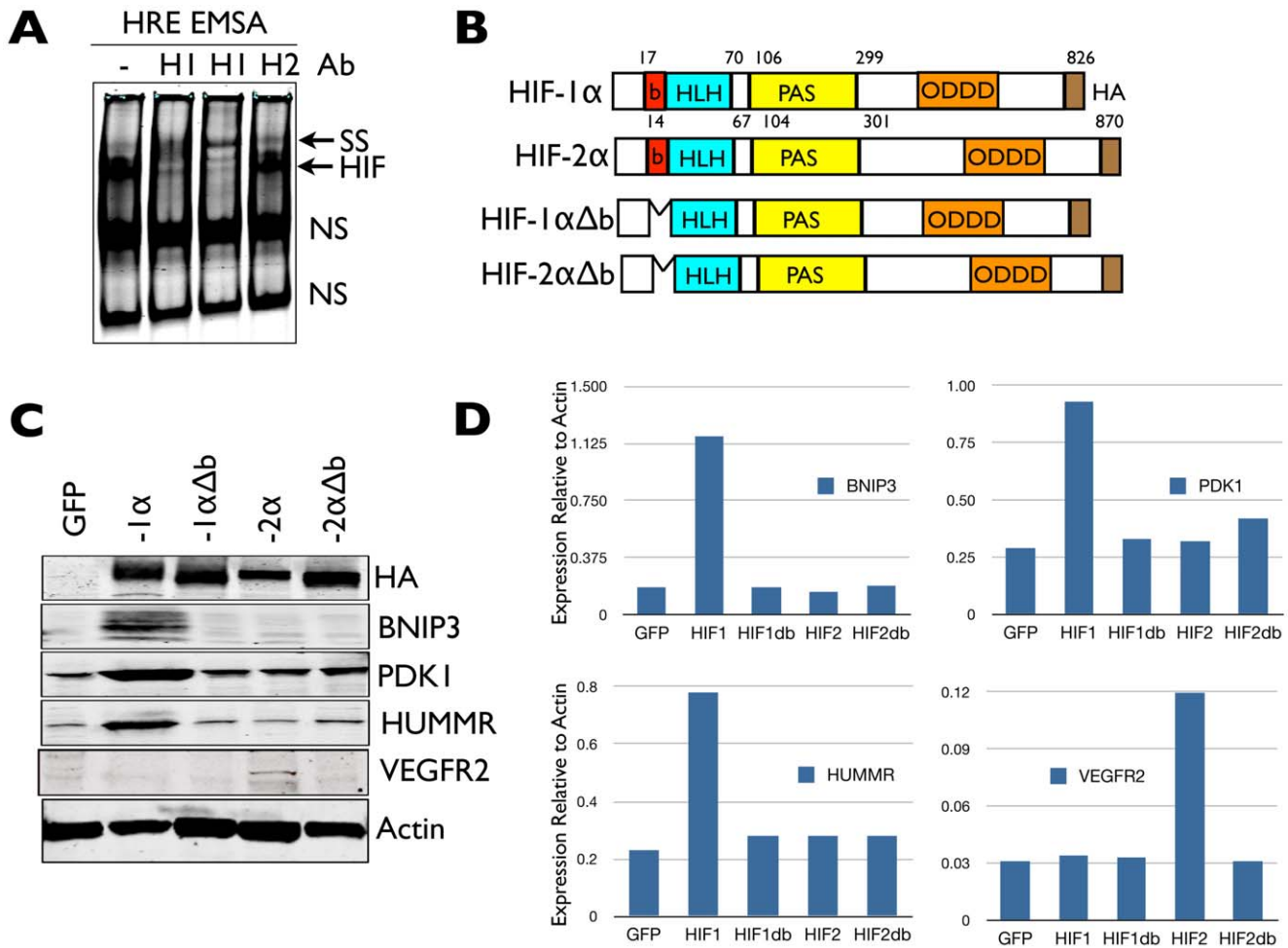


Figure 6. Canonical vs non-canonical HIF target gene-expression in TS cells. (A) Electrophoretic mobility shift assay (EMSA) of differentiated control TGC nuclear extracts with and without 2 different anti-HIF-1 α antibodies (H1) or a HIF-2 α antibody (H2) (“supershift” SS, NS, non-specific complexes.) (B) Schematic representation of full-length HIF-1 α and HIF-2 α , as well as versions lacking their DNA binding basic (b) domains (HLH, Helix-loop-helix, PAS, Per-Arnt-Sim, ODDD, oxygen-dependent degradation domain). (C) Immunoblot detection of stable HA-epitope tagged HIF-1 α , HIF-1 α Δ b, HIF-2 α and HIF-2 α Δ b protein, as well as respective target gene protein products in *Hif-1/2 α ^{-/-}* TSCs. (D) Integrated densitometric quantification of HIF target gene protein products relative to Actin expression in each respective cell line. doi:10.1371/journal.pone.0056949.g006

treated plates or 0.2% gelatin coated glass coverslips, for 7 days. *Vhlh^{+/-}* and *-/-* TSCs were generously provided by M. Celeste Simon (U. Penn). Hypoxia (2% O₂) was produced with the Biospherix XVivo incubator. For differentiation in the presence of inhibitors, TSCs were cultured in plain TSC medium containing either 10 μ M U0126 (Pierce Biotechnology, Rockford, IL), 5 μ M Paclitaxel (Taxol, Calbiochem), 10 μ g/ml Cytochalasin B (Sigma), 60 μ M c-MYC inhibitor (Sigma) or 10 μ M LIMK inhibitor BMS-5 (Synkinase).

Adaptation of TSCs on CELLstart™

For the adaptation of TSCs to the xeno-free substrate CELLstart™ (Invitrogen), cells were passaged from feeder culture using mild trypsinization and plated on CELLstart™ coated tissue culture dishes according to manufacturer’s instructions. Cells were passaged in TSC medium with FGF4 and heparin, but without Fib-CM, upon reaching approximately 75% confluence. Following 5–6 passages, TSC lines on CELLstart™ exhibited a distinct morphology and maintained that morphology for greater than 20 generations in the absence of Fib-CM.

Northern Blot

Northern blot hybridization was performed with the probes for placental lactogen I and 4311 as described previously [17].

Immunoblotting and Immunofluorescence Staining

Whole cell lysates were prepared using a buffer consisting of 150 mM NaCl, 50 mM Tris-HCl (pH 7.4), containing 1 mM EGTA, 1 mM EDTA, 1% Triton X-100, 1% SDS and 10% glycerol. TSCs were incubated with PHEMT buffer (60 mM Pipes, 25 mM Hepes, pH 6.9, 10 mM EGTA, 4 mM MgCl₂ and 0.5% Triton X-100) for 30 min (4°C) and centrifuged to fractionate TSCs into soluble (supernatant) and insoluble fractions (pellet). Immunoblotting was performed with ECL (Amersham) or Odyssey Western blot methodologies and analyzed by Odyssey infrared imaging system (LI-COR Biosciences, Lincoln, NE) using the appropriate secondary antibodies. Briefly, 50–100 μ g of whole cell lysates were run on 7.5–12% SDS-PAGE gel, transferred on PVDF membrane, applied with the primary antibody as indicated. For immunoprecipitation, 500 μ g of whole cell lysates were immunoprecipitated with the indicated antibody and immuno-

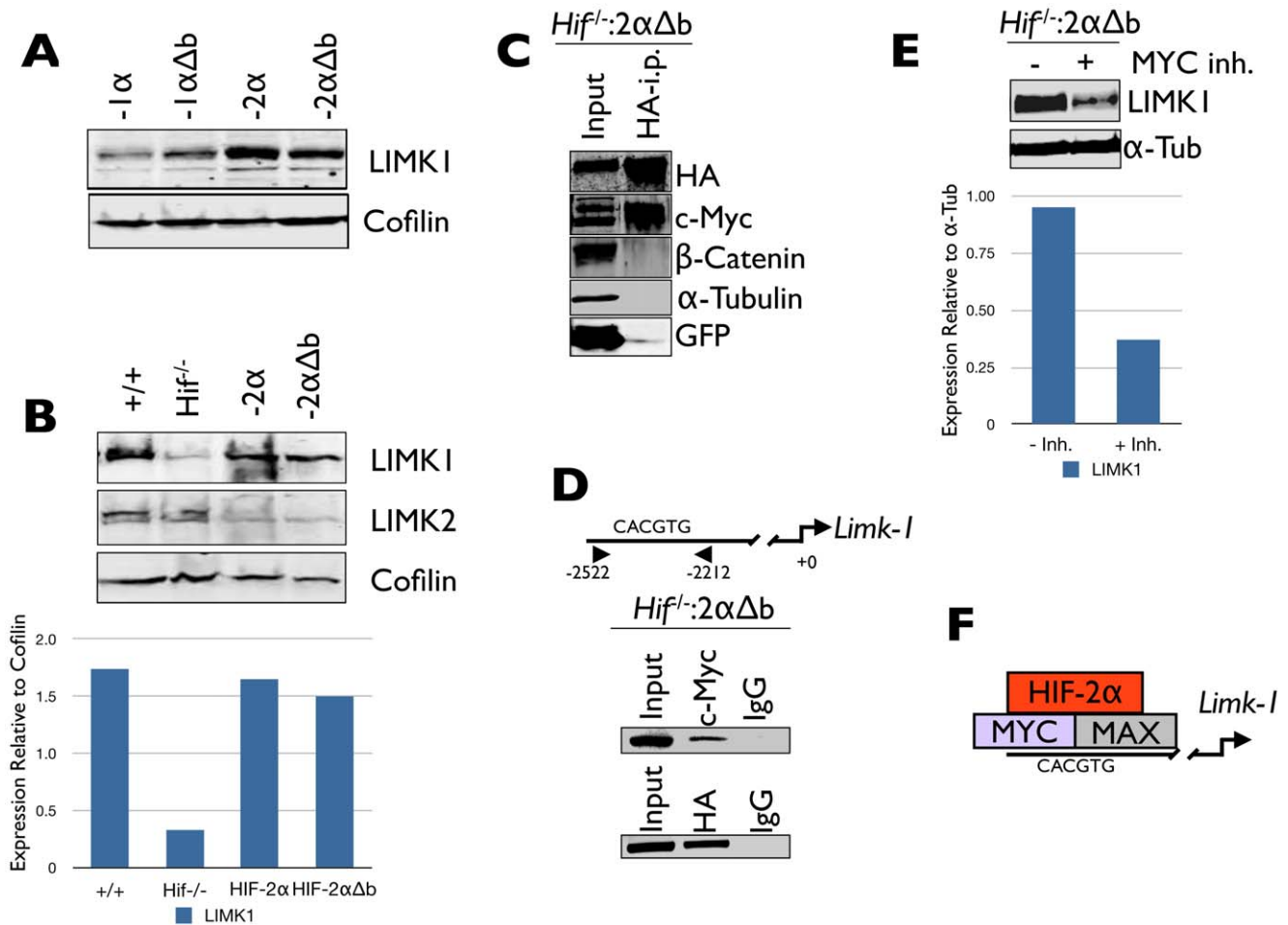


Figure 7. Canonical target gene-independent HIF-2 activity drives LIMK1 expression in TS cells via c-MYC interaction. (A) Immunoblot analysis of LIMK1 protein levels in *Hif-1/2α^{-/-}* TSCs stably reconstituted with full length HIF-1α or -2α, as well as versions lacking their basic domains. (B) Immunoblot analysis of LIMK1 and LIMK2 expression in control (+), *Hif-1/2α^{-/-}* (*Hif^{-/-}*), and HIF-2α and HIF-2αΔb reconstituted *Hif-1/2α^{-/-}* TSCs. Integrated densitometric analysis confirmed that both HIF-2α, as well as HIF-2αΔb, restored LIMK1 expression to control levels in *Hif-1/2α^{-/-}* TSCs. (C) Immunoprecipitation with an anti-HA antibody of HA-tagged HIF-2αΔb followed by immunoblot with anti-HA, c-MYC, β-Catenin, α-Tubulin and GFP antibodies. (D) Schematic representation of E-box element identified within the *Limk-1* promoter. Chromatin immunoprecipitation (ChIP) analysis indicated specific binding of c-MYC and HA-tagged HIF-2αΔb to this element. (E) Immunoblot analysis of LIMK1 protein levels in HIF-2αΔb expressing *Hif-1/2α^{-/-}* TSCs without (-) or with (+) c-MYC inhibitor. Integrated densitometric analysis confirmed reduced expression of LIMK1 relative to α-Tubulin in drug treated cells. (F) Schematic representation of HIF-2α interacting with MYC:MAX heterodimers at the *Limk-1* promoter.

doi:10.1371/journal.pone.0056949.g007

blotted. The following antibodies were used for immunoblotting, EMSA, immunoprecipitation and immunofluorescence staining: CDX2 (Biogenex), EOMES (Orbigen), anti human/mouse HIF-1α (R&D Systems, Minneapolis, MN), HIF-1α c-terminal (Cayman Chemical, Ann Arbor, MI), HIF-2α NB 100–122 (Novus Biologicals), ARNT 2B10 (Abcam, Cambridge, MA), pMAPK3/1 (pERK; Cell Signaling, Danvers, MA), MAPK1(ERK2; Epitomics, Burlingame, CA), α-Tubulin (NeoMarkers, Fremont, CA), Ac-α-Tubulin (Sigma-Aldrich), LIMK1 (BD Biosciences), LIMK2 (Proteintech), Cofilin (BD Biosciences), p-Cofilin (CellSignal), PDK1 (StressGen), BNIP3, VHL M-20, HOPX1 (Santa Cruz Biotechnology, Santa Cruz, CA), β-catenin (Cell Signaling), c-MYC (SCBT), HA (Zymed, South San Francisco, CA), GFP (Aves), E-cadherin (BD Transduction Pharmingen), and HDAC2 (Zymed). Integrated densitometric analysis was performed using Adobe Photoshop.

Immunoprecipitation

Adherent cells were washed twice by addition of ice cold PBS to the monolayer and disposal of the supernatant. 1 ml of freshly made ice cold lysis/wash buffer (50 mM Tris-HCl, 150 mM NaCl pH 7.5, 1% Nonidet P40 0.5% sodium deoxycholate supplemented with 1 complete tablet from Roche) was added to the washed cell monolayers to achieve a concentration of 10⁶–10⁷ cells/ml. Cells were scraped into an eppendorf, and sonicated on ice with 5 pulses each for 8 seconds. Lysate was spun down at 13000 rpm for 5 minutes. Supernatant (except 200 ul) was put onto a new tube. The un-lysed pellet was resuspended into the 200 ul remaining lysate, and sonicated again, the tube centrifuged at 13000rpm for 5 minutes and the new lysate added to the original lysate. 50 ul of this lysate was kept aside as input. To reduce background a pre-clearing step was performed overnight. 50 ul of the homogeneous protein G- agarose (Roche) suspension, equilibrated in the lysis buffer, was added to the 1 ml lysate at 2–8°C on a rotating platform overnight. Beads were then pelleted by centrifugation at

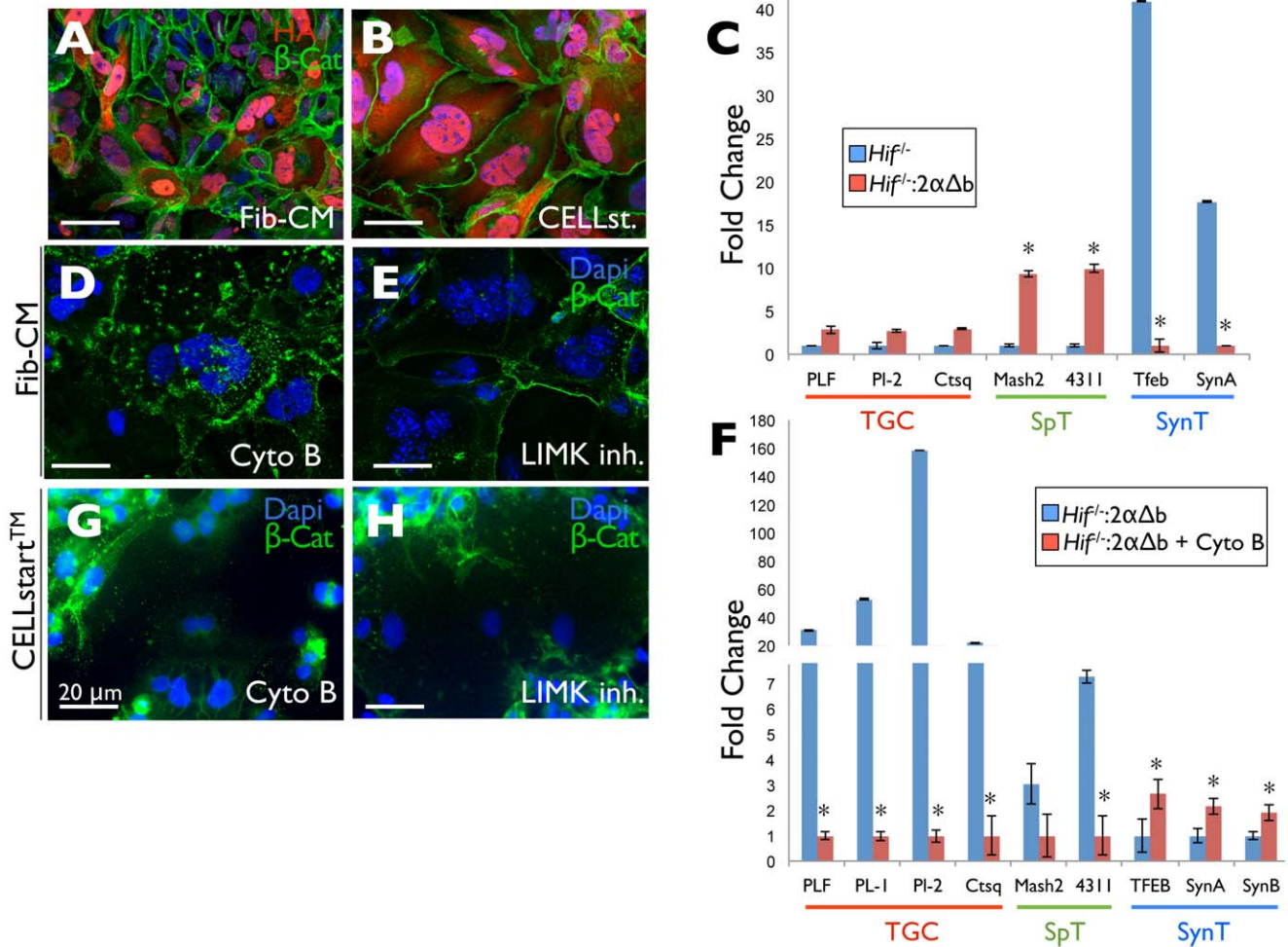


Figure 8. Non-canonical HIF-2-dependent LIMK1 expression promotes TGC formation. Immunofluorescence microscopy of HIF-2αΔb expressing *Hif-1/2α^{-/-}* TSCs differentiated following culture on TC plastic in Fib-CM (A) or on CELLstart™ (B) (green = β-Cat, red = HA). (C) qRT-PCR-based comparison of expression levels of the TGC (PLF, PI-2, Ctsq), spongioroblast (Mash2, 4311) and SynT (Tfeb, SynA) markers in *Hif-1/2α^{-/-}* and HIF-2αΔb reconstituted HIF-null (*Hif^{f/-}:2αΔb*) TSCs differentiated for 7 days following culture on TC plastic in Fib-CM. p values <0.05 versus HIF-null indicated by an asterisk. (D) Immunofluorescence microscopy of HIF-2αΔb expressing *Hif-1/2α^{-/-}* TSCs differentiated following culture on TC plastic in Fib-CM in the presence of Cytochalasin B or (E) the LIMK inhibitor (BMS-5 10 μM)(green = β-Cat). (F) qRT-PCR-based comparison of expression levels of the TGC (PLF, PI-1, PI-2, Ctsq), spongioroblast (Mash2, 4311) and SynT (Tfeb, SynA) markers in HIF-2αΔb reconstituted HIF-null (*Hif^{f/-}:2αΔb*) TSCs differentiated for 7 days following culture on TC plastic in Fib-CM without and with the actin cytoskeleton disrupting agent cytochalasin B (Cyto B). p values <0.05 versus drug free control indicated by an asterisk. (G) Immunofluorescence microscopy of HIF-2αΔb expressing *Hif-1/2α^{-/-}* TSCs differentiated following culture on CellStart™ in the presence of Cytochalasin B or (H) the LIMK inhibitor (BMS-5 10 μM)(green = β-Cat).

doi:10.1371/journal.pone.0056949.g008

2000×g for 2 minutes at 4°C. Supernatant was transferred to a new tube. 50 ul of Agarose-coupled chicken anti-HA (Aves Labs, Inc. Oregon) was equilibrated in the wash/lysis buffer, centrifuged for 2 minutes at 2000×g, and supernatant discarded. The cell lysate was added to these beads and rotated (gentle end-over-end mixing) overnight at 4°C. The lysate/bead complex was then centrifuged for 2 minutes at 2000×g. Pellet was washed 4× by resuspending in lysis/wash buffer. A final wash was performed once for 30 minutes. Beads were then resuspended in 90 ul of 2× SDS sample buffer, boiled for 10 minutes at 95°C. Beads were collected by centrifugation at 2700×g for 2 minutes at 4°C and SDS-PAGE performed with the supernatant.

CHIP Assay

Cells were washed with D-PBS and cross-linked by 1% formaldehyde (37 wt% from Sigma-Aldrich) for 10 min at 37°C.

Glycine (2.5M) was added and incubated in room temperature for 10 minutes. Cells were then washed 3× in D-PBS for 5 minutes and harvested with D-PBS in the presence of protease inhibitor (EDTA-free Complete, Roche Applied Science). These cells were then centrifuged at 3000 rpm for 5 minutes and lysis buffer (1% SDS, 10 mM EDTA, 50 mM Tris-HCl, PH 8.1, with fresh protease inhibitor) was added, sonicated and incubated overnight at 65°C. Rnase A was added and incubated at 37°C, after which 2 ul 0.5 M EDTA, 4 ul 1 M Tris-HCL PH 8.1, 1 ul proteinase K was added and incubated for 2 hours at 45°C to generate 200- to 500-bp DNA fragments, which were subsequently confirmed by agarose gel electrophoresis. Pre-clearing was performed by using 50 ul protein G Sepharose (washed in dilution buffer, 0.01% SDS, 1.1% Triton X-100, 2 mM EDTA, 20 mM Tris-HCl, PH 8.1, 150 mM MgCl2), 30 ul normal IgG, 20 ug salmon sperm and rotated for 2 hours at 4°C. 20 ul was taken as input. Protein G

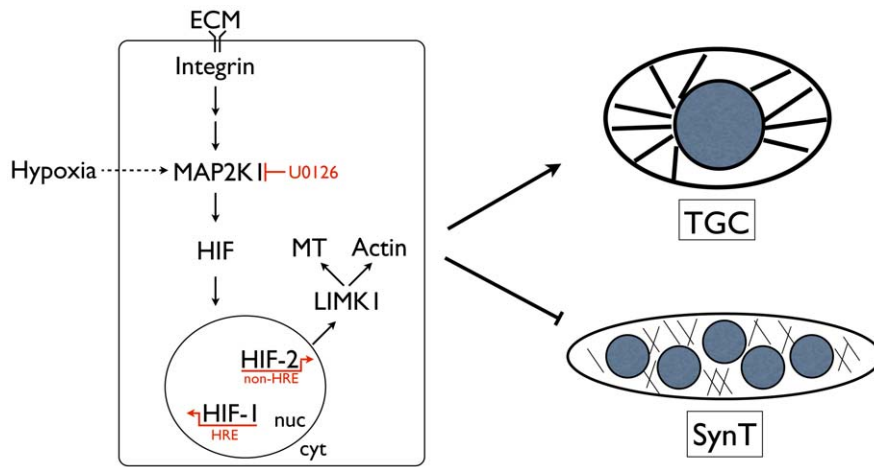


Figure 9. Model of HIF-dependent integration of positional and metabolic cues in the TSC niche. ECM composition regulates HIF stabilization likely downstream of cell surface integrin ligation via MAP2K1/2 activation. Inside-out integrin signaling mechanisms may also be operative. Oxygen sensing and signaling pathways intersect with this signaling cascade to stabilize HIF, when ECM-dependent cues are absent. Stabilized HIF can act via canonical and non-canonical target genes. Non-canonical HIF-2, by interacting with MYC:MAX heterodimers, bind the *Limk1* promoter to activate its expression. LIMK1 promotes microtubule and actin stability, critical for TGC formation, and thereby prevents SynT formation. HIF, therefore, can integrate divergent environmental inputs from within the placenta to regulate cell fate via non-canonical gene expression. doi:10.1371/journal.pone.0056949.g009

sepharose and antibody complexes were prepared by re-suspending protein G with dilution buffer, 1 μ g antibody and incubated on a rotator at 4°C overnight, and then washed twice with dilution buffer and centrifuged at 3000 rpm for 1 minute. Precleared samples were added to the antibody complex beads and rotated at 4°C overnight to collect antibody/antigen/DNA complex. Protein G complex was centrifuged at 3000 rpm for 1 minute, and supernatant removed. Protein G complex was washed sequentially for 5 minutes twice with: low salt buffer (0.1% SDS, 1% Triton X-100, 2 mM EDTA, 150 mM NaCl, 20 mM Tris-HCl, PH 8.1), high salt buffer (0.1% SDS, 1% Triton X-100, 2 mM EDTA, 500 mM NaCl, 20 mM Tris-HCl, PH 8.1), LiCl buffer (0.25 M LiCl, 1% NP-40, 1% deoxycholate, 1 mM EDTA, 10 mM Tris-HCl, PH 8.1), with TE buffer 1 mM EDTA, 10 mM Tris-HCl, PH 8.1). 200 μ l of elution buffer was used containing 20 μ l 10% SDS, 20 μ l 1 M NaHCO₃, 160 μ l H₂O. 100 μ l of elution buffer was added to each tube containing the agarose/antibody complex or the input and incubated in room temperature for 15 minutes. Agarose complex was pelleted by centrifugation (5000 \times g, 1 minute) and supernatant collected. This was repeated with another 100 μ l elution buffer, and added to the first eluate (total volume 200 μ l). Protein/DNA complexes were reversed to free DNA by adding 8 μ l 5 M NaCl, 1 μ l 10 mg/ml RNase A, and incubated at 65°C overnight. DNA was purified by using spin columns from Qiagen. Before purification, 4 μ l 0.5 M EDTA, 8 μ l 1 M Tris-HCl, and 1 μ l protein kinase k was added to each tube and incubated at 45°C for 1 hour. Specifically bound purified DNA fragments were visualized by PCR using specific primers: (forward) 5'-tgcatgcaccctaaataaaaata-3', (reverse) 5'- ccttgaggagcacacataacat-3'.

mRNA Expression Analysis by Real Time PCR

RNA was extracted using TRIzol® Reagent (Invitrogen), and isolation was carried out according to manufacturer's instructions. 2 mcg of RNA per sample was made into cDNA using MMLV reverse transcriptase (Applied Biosystems). Prepared cDNA was amplified using SYBR® Green PCR Master Mix (Life Technologies) and the Bio-Rad iCycler iQ multicolor real time PCR detection system. Cycle threshold (Ct) values were normalized for

amplification using *Hypoxanthine guanine phosphoribosyl transferase (Hprt)*. Data analysis for real time quantitative PCR was done using the deltaCt method. Primer sequences are as follows: *Proliferin (Plf)* Sense – tgaggaatggtcgttgcctt, antisense – tctcatgggctttgtctc. *Placental Lactogen 1 (Pl-1)* Sense – tggttcaagcctactctctt, Antisense – caggggaagtgttctgtctgt. *Placental Lactogen 2 (Pl-2)* Sense – ccaactgtgtgattgtggtgt, Antisense – tcttccgatgttctgtggtg. *Hypoxanthine guanine phosphoribosyl transferase (Hprt)* Sense – aaacaatgcaacttgccttcc, Antisense – ggtcctttaccagcaagct. *Syncytin A (SynA)* Sense – tactcctgcccgatagatga, Antisense – ccgttttcttaacagtggtg. *Syncytin B (SynB)* Sense – ccaccaccatagctcaaaa, Antisense – ggttatagcaggtgcccgaag. *Transcription factor EB (Tfeb)* Sense – aacaaaggcaccatctcaa, Antisense – cagctcggccatattcacac. *Trophoblast specific protein alpha (Tpbpa)*, Sense – cggaaggctcaacatagaa, Antisense – tcaaatcagggtcatcaacaa. *Mammalian achaete-scute homolog 2 (Mash2)* Sense – TTTTCGAGGACGCAATAAGC, Antisense – cactgtctcaggactcccta. Statistical analysis of real time PCR results were performed as follows: All data points were performed in triplicate. One-way analysis of variance of the results was performed in Microsoft Excel 2007 to determine the presence of significant differences within the data sets. When analysis of variance indicated that a significant difference may be present, a two-sample Student's t-test was performed to compare experimental data with appropriate controls [77]. Statistical significance was determined at a value of P<0.05 and is represented with an asterisk.

Plasmid Constructs and Ectopic Expression

The full-length open reading frame of Hif-1 α and Hif-2 α were PCR amplified from cDNA constructs. Deletional mutants were generated removing the basic domain, Hif-1 α Δ b (deletion of amino acids 4–27) and Hif-2 α Δ b (deletion of amino acids 6–24) by high fidelity PCR. All expression constructs were modified to include the 9 amino acid hemagglutinin epitope YPYDVPDYA fused directly to the C-terminus and cloned into the ENTRD-TOPO vector (Invitrogen). The integrity of the constructs was confirmed by DNA sequencing. For expression in cell culture, a derivative of the Piggybac transposon system was employed allowing high efficiency expression. The parental plasmid EBXN

containing the minimal Piggybac 5' and 3' inverted terminal repeats as well as a CMV enhancer chicken Beta-actin promoter expression cassette was modified to include the SV40 promoter Blasticidin cassette allowing for eukaryotic selection in cell culture. The plasmid was further modified to include the Invitrogen Gateway Rfa cassette allowing for phiC31 mediated recombination. For monitoring transfection efficiency, EMCV IRES upstream of palmitoylated EGFP was inserted, PBX2.2. A control construct containing monomeric EGFP (Karel Svoboda, Addgene Plasmid 18696) was inserted into the parental plasmid PBX2.1.

Transfection of TSC lines was performed with Lipofectamine LTX and PLUS reagent (Invitrogen) in placental fibroblast-free culture. A 2:1 molar ratio of Piggybac transposase helper plasmid, PB, was combined with the transposon expression construct to mediate integration and high level expression. Selection with Blasticidin 5 mcg/ml was performed to identify stable integrants, which were subsequently passaged on placental fibroblasts.

References

- Simon MC, Keith B (2008) The role of oxygen availability in embryonic development and stem cell function. *Nat Rev Mol Cell Biol* 9: 285–296.
- Semenza GL (2009) Regulation of oxygen homeostasis by hypoxia-inducible factor 1. *Physiology (Bethesda)* 24: 97–106.
- Kaelin WG Jr, Ratcliffe PJ (2008) Oxygen sensing by metazoans: the central role of the HIF hydroxylase pathway. *Mol Cell* 30: 393–402.
- Wang GL, Jiang BH, Rue EA, Semenza GL (1995) Hypoxia-inducible factor 1 is a basic-helix-loop-helix-PAS heterodimer regulated by cellular O₂ tension. *Proc Natl Acad Sci U S A* 92: 5510–5514.
- Chandel NS, Maltepe E, Goldwasser E, Mathieu CE, Simon MC, et al. (1998) Mitochondrial reactive oxygen species trigger hypoxia-induced transcription. *Proc Natl Acad Sci U S A* 95: 11715–11720.
- Dunwoodie SL (2009) The role of hypoxia in development of the Mammalian embryo. *Dev Cell* 17: 755–773.
- Ryan HE, Lo J, Johnson RS (1998) HIF-1 alpha is required for solid tumor formation and embryonic vascularization. *Embo J* 17: 3005–3015.
- Iyer NV, Kotch LE, Agani F, Leung SW, Laughner E, et al. (1998) Cellular and developmental control of O₂ homeostasis by hypoxia-inducible factor 1 alpha. *Genes Dev* 12: 149–162.
- Maltepe E, Schmidt JV, Baunoch D, Bradfield CA, Simon MC (1997) Abnormal angiogenesis and responses to glucose and oxygen deprivation in mice lacking the protein ARNT. *Nature* 386: 403–407.
- Cowden Dahl KD, Fryer BH, Mack FA, Compennolle V, Maltepe E, et al. (2005) Hypoxia-inducible factors 1alpha and 2alpha regulate trophoblast differentiation. *Mol Cell Biol* 25: 10479–10491.
- Kozak KR, Abbott B, Hankinson O (1997) ARNT-deficient mice and placental differentiation. *Dev Biol* 191: 297–305.
- Adelman DM, Gertsenstein M, Nagy A, Simon MC, Maltepe E (2000) Placental cell fates are regulated in vivo by HIF-mediated hypoxia responses. *Genes Dev* 14: 3191–3203.
- Maltepe E, Bakardjiev AI, Fisher SJ (2012) The placenta: transcriptional, epigenetic, and physiological integration during development. *J Clin Invest* 120: 1016–1025.
- Rossant J, Cross JC (2001) Placental development: lessons from mouse mutants. *Nat Rev Genet* 2: 538–548.
- Watson ED, Cross JC (2005) Development of structures and transport functions in the mouse placenta. *Physiology (Bethesda)* 20: 180–193.
- Tanaka S, Kunath T, Hadjantonakis AK, Nagy A, Rossant J (1998) Promotion of trophoblast stem cell proliferation by FGF4. *Science* 282: 2072–2075.
- Maltepe E, Krampitz GW, Okazaki KM, Red-Horse K, Mak W, et al. (2005) Hypoxia-inducible factor-dependent histone deacetylase activity determines stem cell fate in the placenta. *Development* 132: 3393–3403.
- Zheng QA, Chang DC (1991) Reorganization of cytoplasmic structures during cell fusion. *J Cell Sci* 100 (Pt 3): 431–442.
- Shibukawa Y, Yamazaki N, Kumasawa K, Daimon E, Tajiri M, et al. (2012) Calponin 3 Regulates Actin Cytoskeleton Rearrangement in Trophoblastic Cell Fusion. *Mol Biol Cell*.
- Yoshie M, Kashima H, Bessho T, Takeichi M, Isaka K, et al. (2008) Expression of stathmin, a microtubule regulatory protein, is associated with the migration and differentiation of cultured early trophoblasts. *Hum Reprod* 23: 2766–2774.
- Gauster M, Siwetz M, Orendi K, Moser G, Desoye G, et al. (2012) Caspases rather than calpains mediate remodelling of the fodrin skeleton during human placental trophoblast fusion. *Cell Death Differ* 17: 336–345.
- Swistowski A, Peng J, Han Y, Swistowska AM, Rao MS, et al. (2009) Xeno-free defined conditions for culture of human embryonic stem cells, neural stem cells and dopaminergic neurons derived from them. *PLoS One* 4: e6233.

Acknowledgments

We thank Susan Fisher, Olga Genbacev, Anna Bakardjiev and Kevin Shannon (UCSF) for reagents and thoughtful discussion of the manuscript and M. Celeste Simon (Abramson Cancer Research Institute, UPenn) for *Vhlh^{-/-}* TSCs. We thank Torsten Wittmann (UCSF) for help with confocal microscopy and thoughtful discussion, Natalie Ahn (HHMI, UC Boulder) for MAP2K1 constructs, Michael Olson (Beatson institute for Cancer Research, Glasgow) for LIMK1 constructs and MK Tee (WL Miller Lab, UCSF) for assistance with genomics analyses. The contents of this publication are solely the responsibility of the authors and do not necessarily represent the official views of CIRM or any other agency of the State of California.

Author Contributions

Conceived and designed the experiments: HJC TAS EM PFR. Performed the experiments: HJC TAS KVT KA JDT AMP JG AMR XL DMQ. Analyzed the data: HJC KVT PFR EM. Wrote the paper: EM.

44. Scott RW, Hooper S, Crighton D, Li A, Konig I, et al. (2012) LIM kinases are required for invasive path generation by tumor and tumor-associated stromal cells. *J Cell Biol* 191: 169–185.
45. Ross-Macdonald P, de Silva H, Guo Q, Xiao H, Hung CY, et al. (2008) Identification of a nonkinase target mediating cytotoxicity of novel kinase inhibitors. *Mol Cancer Ther* 7: 3490–3498.
46. Guilak F, Cohen DM, Estes BT, Gimble JM, Liedtke W, et al. (2009) Control of stem cell fate by physical interactions with the extracellular matrix. *Cell Stem Cell* 5: 17–26.
47. Kim SH, Turnbull J, Guimond S (2012) Extracellular matrix and cell signalling: the dynamic cooperation of integrin, proteoglycan and growth factor receptor. *J Endocrinol* 209: 139–151.
48. Votteler M, Kluger PJ, Walles H, Schenke-Layland K (2012) Stem cell microenvironments—unveiling the secret of how stem cell fate is defined. *Macromol Biosci* 10: 1302–1315.
49. Eshghi S, Voglezang MG, Hynes RO, Griffith LG, Lodish HF (2007) Alpha4beta1 integrin and erythropoietin mediate temporally distinct steps in erythropoiesis: integrins in red cell development. *J Cell Biol* 177: 871–880.
50. Skuli N, Monferran S, Delmas C, Favre G, Bonnet J, et al. (2009) Alpha4beta3/alpha5beta1 integrins-FAK-RhoB: a novel pathway for hypoxia regulation in glioblastoma. *Cancer Res* 69: 3308–3316.
51. Cowden Dahl KD, Robertson SE, Weaver VM, Simon MC (2005) Hypoxia-inducible factor regulates alpha4beta3 integrin cell surface expression. *Mol Biol Cell* 16: 1901–1912.
52. Wang J, Armant DR (2002) Integrin-mediated adhesion and signaling during blastocyst implantation. *Cells, tissues, organs* 172: 190–201.
53. Sutherland A (2003) Mechanisms of implantation in the mouse: differentiation and functional importance of trophoblast giant cell behavior. *Dev Biol* 258: 241–251.
54. Rosario GX, Konno T, Soares MJ (2008) Maternal hypoxia activates endovascular trophoblast cell invasion. *Dev Biol* 314: 362–375.
55. Ramos JW (2008) The regulation of extracellular signal-regulated kinase (ERK) in mammalian cells. *Int J Biochem Cell Biol* 40: 2707–2719.
56. Hsu JC, Perrimon N (1994) A temperature-sensitive MEK mutation demonstrates the conservation of the signaling pathways activated by receptor tyrosine kinases. *Genes Dev* 8: 2176–2187.
57. Wu Y, Han M, Guan KL (1995) MEK-2, a *Caenorhabditis elegans* MAP kinase, functions in Ras-mediated vulval induction and other developmental events. *Genes Dev* 9: 742–755.
58. Umbhauer M, Marshall CJ, Mason CS, Old RW, Smith JC (1995) Mesoderm induction in *Xenopus* caused by activation of MAP kinase. *Nature* 376: 58–62.
59. Kornfeld K, Guan KL, Horvitz HR (1995) The *Caenorhabditis elegans* gene mek-2 is required for vulval induction and encodes a protein similar to the protein kinase MEK. *Genes Dev* 9: 756–768.
60. Hamanaka RB, Chandel NS (2009) Mitochondrial reactive oxygen species regulate hypoxic signaling. *Curr Opin Cell Biol* 21: 894–899.
61. Harburger DS, Calderwood DA (2009) Integrin signalling at a glance. *J Cell Sci* 122: 159–163.
62. Bissonauth V, Roy S, Gravel M, Guillemette S, Charron J (2006) Requirement for Map2k1 (Mek1) in extra-embryonic ectoderm during placentogenesis. *Development* 133: 3429–3440.
63. Saba-El-Leil MK, Vella FD, Vernay B, Voisin L, Chen L, et al. (2003) An essential function of the mitogen-activated protein kinase Erk2 in mouse trophoblast development. *EMBO Rep* 4: 964–968.
64. Hatano N, Mori Y, Oh-hora M, Kosugi A, Fujikawa T, et al. (2003) Essential role for ERK2 mitogen-activated protein kinase in placental development. *Genes Cells* 8: 847–856.
65. Giroux S, Tremblay M, Bernard D, Cardin-Girard JF, Aubry S, et al. (1999) Embryonic death of Mek1-deficient mice reveals a role for this kinase in angiogenesis in the labyrinthine region of the placenta. *Curr Biol* 9: 369–372.
66. Nadeau V, Guillemette S, Belanger LF, Jacob O, Roy S, et al. (2009) Map2k1 and Map2k2 genes contribute to the normal development of syncytiotrophoblasts during placentation. *Development* 136: 1363–1374.
67. Galabova-Kovacs G, Matzen D, Piazzolla D, Meissl K, Plyushch T, et al. (2006) Essential role of B-Raf in ERK activation during extraembryonic development. *Proc Natl Acad Sci U S A* 103: 1325–1330.
68. Dubois NC, Adolphe C, Ehninger A, Wang RA, Robertson EJ, et al. (2008) Placental rescue reveals a sole requirement for c-Myc in embryonic erythroblast survival and hematopoietic stem cell function. *Development* 135: 2455–2465.
69. Fukuda R, Hirota K, Fan F, Jung YD, Ellis LM, et al. (2002) Insulin-like growth factor 1 induces hypoxia-inducible factor 1-mediated vascular endothelial growth factor expression, which is dependent on MAP kinase and phosphatidylinositol 3-kinase signaling in colon cancer cells. *J Biol Chem* 277: 38205–38211.
70. Lee SH, Che X, Jeong JH, Choi JY, Lee YJ, et al. (2012) Runx2 protein stabilizes hypoxia-inducible factor-1alpha through competition with von Hippel-Lindau protein (pVHL) and stimulates angiogenesis in growth plate hypertrophic chondrocytes. *J Biol Chem* 287: 14760–14771.
71. Escuin D, Kline ER, Giannakakou P (2005) Both microtubule-stabilizing and microtubule-destabilizing drugs inhibit hypoxia-inducible factor-1alpha accumulation and activity by disrupting microtubule function. *Cancer Res* 65: 9021–9028.
72. Mabejess NJ, Escuin D, LaVallee TM, Pribluda VS, Swartz GM, et al. (2003) 2ME2 inhibits tumor growth and angiogenesis by disrupting microtubules and dysregulating HIF. *Cancer Cell* 3: 363–375.
73. Burton GJ (2009) Oxygen, the Janus gas; its effects on human placental development and function. *J Anat* 215: 27–35.
74. Pringle KG, Kind KL, Sferruzzi-Perri AN, Thompson JG, Roberts CT (2009) Beyond oxygen: complex regulation and activity of hypoxia inducible factors in pregnancy. *Hum Reprod Update*.
75. Zhang L, Luo J, Wan P, Wu J, Laski F, et al. (2012) Regulation of cofilin phosphorylation and asymmetry in collective cell migration during morphogenesis. *Development* 138: 455–464.
76. Karthikeyan VJ, Lane DA, Beevers DG, Lip GY, Blann AD (2012) Matrix metalloproteinases and their tissue inhibitors in hypertension-related pregnancy complications. *J Hum Hypertens*.
77. Rieu I, Powers SJ (2009) Real-time quantitative RT-PCR: design, calculations, and statistics. *Plant Cell* 21: 1031–1033.